Monte Carlo simulation of impact-ionization-induced breakdown and current filamentation in δ-doped GaAs

B. Kehrer, W. Quade, and E. Schöll
Institut für Theoretische Physik, Technische Universität Berlin, Hardenbergstrasse 36, 10623 Berlin, Germany
(Received 18 October 1994)

We present Monte Carlo simulations of impact-ionization-induced impurity breakdown in n-GaAs at 4.2 K with dopants arranged in parallel monoatomic planes (δ doping). S-shaped current-field characteristics are obtained by a direct single-particle Monte Carlo simulation for homogeneously doped material. For δ-doped GaAs we calculate the spatial distribution of the carrier density, mean electron energy, and space-charge field self-consistently as a function of time by a weighted ensemble Monte Carlo method. For initial values on the low-conductivity branch of the S-shaped characteristics we find that current filaments centered around the δ-doped layers are formed. Our simulations explain the experimentally observed shrinking of the bistable regime as well as its shift to lower voltages as compared to homogeneous material.

I. INTRODUCTION

Impurity breakdown in homogeneously doped semiconductors has been widely studied both from the theoretical and experimental points of view.[1,2] At liquid-helium temperatures these materials show an abrupt nonequilibrium phase transition between a low and a high conductivity state if a certain threshold of the applied electric field is exceeded.[2] The autocatalytic key process for this breakdown is impact ionization of shallow impurities, leading to an avalanchelike increase of the free carrier density. Depending on the experimental conditions, either monotonic or S-shaped current-field characteristics may occur. The latter often give rise to complex dynamical behavior, such as breathing or chaotically oscillating current filaments.[3-9]

The dopants play a crucial role in impurity breakdown. They not only serve as centers for the generation-recombination kinetics of the charge carriers but also influence the carrier distribution function by ionized impurity scattering. While the influence of spatially homogeneous concentrations of donors and acceptors on the current-field characteristics is well known,[2] the question of whether bistability is also affected by partial ordering of the dopants has not been studied until recently. Kostial *et al.*[10] experimentally investigated the impurity breakdown in molecular-beam epitaxy-grown GaAs samples where the donors (Si) were ordered in monoatomic planes (δ doping). The acceptors were either ordered in δ layers too or randomly distributed in the volume. It was found that the current-field characteristics remains S shaped if the concentration of donors in the δ layer is less than 10^{11} cm^{-2}, but both the threshold voltage and the width of the bistability interval were affected.

Here we perform Monte Carlo (MC) simulations in order to get insight into the role of partial ordering of dopants on impurity breakdown and current filamentation. Because the slow time scales on which the generation-recombination (GR) processes take place are many orders of magnitude slower than those of the microscopic scattering processes, a full dynamical simulation of the relaxation to steady state is beyond the present possibilities. To overcome these difficulties we adopt the following strategy. First we determine the static S-shaped current-field characteristic for equivalently doped homogeneous material by a single-particle MC simulation. In a second step all donors are assumed to be in a small layer in the middle of the simulated sample, representing the δ-doped plane. Using the stationary values for carrier densities and electron temperatures obtained for the homogeneous sample as an initial condition within the δ-doped layer, we calculate self-consistently the spatial distributions of free carrier density, mean electron energy, and lateral electric field in the δ-doped sample by an ensemble Monte Carlo (EMC) simulation.

The S-shaped current-field characteristics as well as the oscillatory and filamentary instabilities in bulk semiconductors have been qualitatively modeled on the basis of classical rate equations with simple phenomenological transport coefficients.[2,11-13] In order to obtain a more detailed quantitative understanding, a microscopic simulation of the generation-recombination and transport parameters is required. That has been done for the case of homogeneously doped p-Ge at 4 K by means of single-particle[14] or many-particle[15] MC simulations. The generation-recombination kinetics, involving in particular impact ionization from shallow acceptor levels, has been modeled in terms of a single acceptor level[14] or two acceptor levels[15] (ground and excited state), respectively. Following a common approach, the GR coefficients in dependence on the electric field obtained from the MC data can be fitted by smooth analytical functions and substituted into the macroscopic space- and time-dependent differential equations describing the nonlinear spatiotemporal dynamics of the carrier densities and the electric field. In this way the complex dynamics of current filaments in the regime of low-temperature impurity breakdown in p-Ge has been adequately described on a

0163-1829/95/51(12)/7725(9)/$06.00 ©1995 The American Physical Society

level which links the microscopic physics and the macroscopic nonlinear dynamics.[8]

In this paper we present an entirely microscopic simulation of the nonlinear GR and transport processes in homogeneously and inhomogeneously doped n-GaAs at 4.2 K. We extend the method previously used for Ge (Ref. 14) by implementing both ground and excited impurity levels into a single-particle MC simulator. This enables us to obtain a direct MC simulation of the bistable S-shaped characteristics including a negative differential conductivity (SNDC) branch, which was not possible with the approaches in Refs. 14 and 15. The MC data for GR and impact ionization rates, impurity level occupation, drift velocity, electron temperature, momentum, and energy relaxation times offer detailed insight into the mechanism of impurity breakdown in n-GaAs. Furthermore, we directly simulate spatially inhomogeneous situations and thus are able to reproduce current filamentation without the aid of macroscopic space- and time-dependent balance equations as used in Refs. 8 and 15. In contrast to Refs. 8 and 15, here the current filaments are not purely self-organized through GR processes, but are strongly determined by the space charges of the inhomogeneously distributed donors and compensating acceptors. A preliminary account of some results has been given in Ref. 16. Monte Carlo simulations of impurity impact ionization in bulk GaAs have also been performed by van Hall and Zwaal,[17] but no SNDC was obtained. Other microscopic approaches, based on cellular automata, have also been applied to nonlinear transport in bulk GaAs.[18] Their virtue lies in the fact that they can deal with complicated boundary conditions, albeit at the expense of a coarse-grained **k** space.

The paper is organized as follows. In Sec. II we introduce the single-particle MC simulator. In Sec. III we apply it to homogeneously doped GaAs and calculate its SNDC transport properties. In Sec. IV the weighted ensemble MC method, which is used for δ-doped GaAs, is described. In Sec. V the current filaments are directly calculated with the EMC method, using the data from Sec. III as initial conditions. Finally, in Sec. VI some conclusions are drawn.

II. THE MONTE CARLO METHOD FOR HOMOGENEOUS n-GaAs

Our starting point is a standard one-particle MC simulator[14,19,20] based on the ergodicity of the system, which simulates stationary, spatially homogeneous situations. The simulated particle is subjected to successive scattering processes. In n-GaAs at 4 K the relevant intraband scattering processes are elastic ionized impurity scattering (Conwell-Weisskopf approximation) and inelastic acoustic deformation potential scattering. Optical phonon scattering is neglected because of the low lattice temperature, although optical phonon emission becomes relevant for energies above 36 meV.[21] However, those states are not frequently populated except at the highest fields. Generation-recombination processes involving the conduction band and the shallow donors account for the switching between a low and a high conductivity state. Since the experimentally observed bistability in the transition regime can be explained in terms of standard GR kinetics only if at least two impurity levels are taken into account,[11,22] we model the infinite hydrogenlike energy spectrum of the shallow donors by the ground state and an "effective" excited state[23] close to the band edge. In particular, we include impact ionization from both the ground state and the excited donor level. The inverse process, Auger recombination, can be neglected for low carrier densities.

Impact ionization from both the donor ground state and the effective excited state is described by a recent model which extends the Keldysh model[24] by including the wave vector dependence of the Coulomb matrix element and therefore exhibits the correct asymptotic behavior of the microscopic scattering rate at high energies.[15] Furthermore, energy loss through impact ionization is fully taken into account in the simulation. Recombination assisted by acoustic phonons is approximated by Lax's "cascade capture" model.[25,26] After being trapped, the simulated particle is immediately regenerated with a **k** vector randomly distributed on an energy sphere at energy E corresponding to the probability of thermal generation $P_{\text{gen}}(E)$.[14,27] Figure 1 shows the microscopic scattering rates the simulated particle is subjected to. The plot is scaled such that the carrier concentrations chosen refer to a situation at thermodynamic equilibrium, corresponding to the stationary distribution for a simulated electric field $\mathcal{E} = 0$.

The microscopic rates of all band-impurity processes depend on the carrier concentration in the band and impurity states, which in turn depend on the distribution function in the steady state. To obtain these stationary concentrations, the MC method has to be combined self-consistently with rate equations expressing particle conservation:

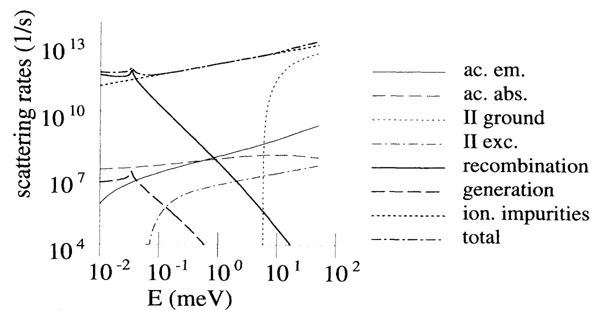

FIG. 1. Microscopic scattering rates as a function of the carrier energy used in the Monte Carlo simulation: emission (ac. em.) and absorption (ac. abs.) of acoustic phonons, impact ionization from the ground (II ground) and the excited (II exc.) level, thermal generation and capture, and ionized impurity scattering (ion. impurities). These rates are calculated for electrons in n-GaAs at a lattice temperature of 4.2 K (see Table I).

$$\dot{n} = X_1^S n_{t_2} - T_1^{S^{\rm MC}}(n, n_{t_1}, n_{t_2}, \mathcal{E}) n p_t + X_1^{\rm MC}(n, n_{t_1}, n_{t_2}, \mathcal{E}) n n_{t_1} + X_1^{*^{\rm MC}}(n, n_{t_1}, n_{t_2}, \mathcal{E}) n n_{t_2}, \quad (1)$$

$$\dot{n}_{t_1} = -X^* n_{t_1} + T^* n_{t_2} - X_1^{\rm MC}(n, n_{t_1}, n_{t_2}, \mathcal{E}) n n_{t_1}, \quad (2)$$

$$\dot{n}_{t_2} = -\dot{n} - \dot{n}_{t_1}. \quad (3)$$

Here n_{t_1}, n_{t_2} are the carrier concentrations in the donor ground and excited state, respectively, and n is the concentration of conduction electrons. X_1^S is the rate coefficient of thermal ionization of the excited donor state, $T_1^{S^{\rm MC}}$ is the capture coefficient of the excited donor state, and $X_1^{\rm MC}, X_1^{*^{\rm MC}}$ are the coefficients for impact ionization from the ground and the excited state, respectively. T^* and X^* describe relaxation of the donor excited state to the ground state and its reverse process, respectively. Also the condition of charge neutrality $n_{t_1} + n_{t_2} + n = N_D - N_A$ must be fulfilled in the uniform state. N_D is the donor concentration, N_A the concentration of compensating acceptors ($N_A < N_D$), and $p_t = N_A + n$ is the concentration of ionized donors. The superscript MC refers to the fact that those GR coefficients depend on the nonequilibrium steady-state distribution function and therefore have to be calculated self-consistently from the MC simulation by averaging the microscopic transition probabilities over the nonequilibrium distribution function $f(\mathbf{k})$, which depends parametrically on the carrier densities n,n_{t_1},n_{t_2} and the electric field $\mathcal{E}$:

$$X_1^{*^{\rm MC}}(n, n_{t_1}, n_{t_2}, \mathcal{E}) = \frac{1}{n n_{t_2}} \int d^3k f(\mathbf{k}; n, n_{t_1}, n_{t_2}, \mathcal{E}) P_{ii}^{t_2}(\mathbf{k}, n_{t_2}), \quad (4)$$

$$X_1^{\rm MC}(n, n_{t_1}, n_{t_2}, \mathcal{E}) = \frac{1}{n n_{t_1}} \int d^3k f(\mathbf{k}; n, n_{t_1}, n_{t_2}, \mathcal{E}) P_{ii}^{t_1}(\mathbf{k}, n_{t_1}), \quad (5)$$

$$T_1^{S^{\rm MC}}(n, n_{t_1}, n_{t_2}, \mathcal{E}) = \frac{1}{n p_t} \int d^3k f(\mathbf{k}; n, n_{t_1}, n_{t_2}, \mathcal{E}) P_{\rm rec}(\mathbf{k}, p_t), \quad (6)$$

where $P_{ii}^{t_2}$, $P_{ii}^{t_1}$, and $P_{\rm rec}$ are the microscopic impact ionization rates of the excited state, the ground state, and the capture rate, respectively, as shown in Fig. 1 and derived in Refs. 15, 25, and 26. Unlike in the simple phenomenological theory,[2] the MC GR coefficients thus depend parametrically on n, n_{t_1}, and n_{t_2}. During each step of the MC simulation those concentrations are kept constant. If one neglects the Poole-Frenkel effect, X_1^S, X^*, and T^* are independent of the conduction band distribution function and can be substituted by their equilibrium values.

A two-level iteration procedure is used to solve the above problem. In a first step we keep n fixed in the MC simulation and determine the n-dependent GR coefficients with a starting value of n_{t_2}/n_{t_1}. Iteratively the steady state occupation ratio n_{t_2}/n_{t_1} is calculated by a fixed point method, according to

$$\frac{n_{t_2}}{n_{t_1}} = \frac{X_1^{\rm MC}(n, n_{t_1}, n_{t_2}, \mathcal{E}) n + X^*}{T^*}, \quad (7)$$

which is obtained from Eqs. (1)–(3). Starting from an arbitrary value for n_{t_2}/n_{t_1} as the input parameter, the simulation yields a value for $X_1^{\rm MC}$ which can be used to evaluate an improved value for n_{t_2}/n_{t_1}. This iterative procedure is repeated until convergence is reached, which typically occurs after about 5–10 iteration steps. Then the value for n is increased and the above procedure is repeated. Given the dependence of the GR coefficients on the concentration of free carriers n, the stationary values for n can be determined from Eqs. (1)–(3). The procedure can best be explained with the help of Fig. 2, where the sum of all generation rates and the total recombination rate from (1) are shown as a function of n. The stationary values for n are given by the intersections of the two curves. As is evident from the figure, there are three steady states, only two of which are stable, corresponding to the low and the high conductivity branch of the SNDC characteristics. This is in good agreement with the phenomenological theory; see Fig. 2.14 in Ref. 2. It should be stressed that this method allows us to investigate stationary carrier distributions which are dynamically unstable against fluctuations; this is not possible, e.g., with a standard EMC method, which follows the distribution function dynamically. In conclusion, our simulation yields detailed information on the dependence of the GR coefficients upon n and $\mathcal{E}$, which is not available in less sophisticated approaches, but which is crucial for correctly describing SNDC.

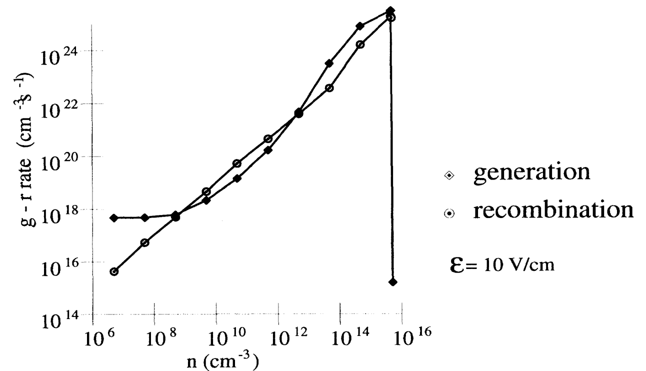

FIG. 2. Generation and recombination rates versus the concentration of free electrons for constant electric field ($\mathcal{E}$ = 10 V/cm). The three intersections represent stationary points.

III. IMPURITY BREAKDOWN IN HOMOGENEOUSLY DOPED GaAs

We have performed simulations for n-GaAs with a parabolic isotropic conduction band. Table I shows the material parameters of the simulation. The microscopic scattering rates are normalized such that the thermodynamic equilibrium values for the GR coefficients (denoted by the superscript 0) are matched. T_1^{S0}, X_1^{S0}, X^*, and T^* are chosen according to experimental data,[28] X_1^{*0} is determined by averaging the microscopic probability for impact ionization from the *first* excited state.[15]

Figure 3 shows the simulated stationary values of the mean electron energy kT_e, the drift velocity v_D, the carrier densities in the conduction band n and in donor states n_{t_1} (ground state) and n_{t_2} (excited state), the momentum and energy relaxation times, the GR coefficients, and the mobility obtained from the MC simulation as a function of the electric field $\mathcal{E}$. In agreement with the phenomenological theory,[2] we observe a regime where one value of the electric field corresponds to three values of n. This behavior leads to an S-shaped current-field characteristic (SNDC) (Fig. 4).

The mechanism leading to SNDC can be studied in detail if the GR rates are compared for various values of n at a given electric field (Fig. 2). The points of intersection of these two rates represent stationary points. The stationary occupation ratio n_{t_1}/n_{t_2} together with the condition of charge neutrality has been used to eliminate the occupation of donor states. For low values of n the generation rate is dominated by thermal generation, as in the phenomenological theory.[2,11] For higher values of n the increasing occupation of excited state through impact ionization from the ground state leads to a stronger than linear increase of the generation rate with n, induced by impact ionization from the excited state. If n is close to the effective donor concentration, impact ionization sharply decreases again because all the donor states are depleted. This is also reflected in the behavior of n_{t_1} and n_{t_2} as a function of field [Fig. 3(b)]. The occupation of the excited state n_{t_2} shows an S-shaped increase at the onset of impact ionization, but for higher fields on the upper branch decreases again. At the same point the occupation of the ground state n_{t_1} sharply drops and falls below that of the excited state.

The impact ionization coefficients X_1 and X_1^* as well as the capture coefficient T_1^S have been calculated from the MC steady-state nonequilibrium distribution function according to Eqs. (4)–(6) [Figs. 3(c) and 3(d)]. Those coefficients depend not only on the electric field, but also upon the carrier concentration n and are therefore double valued if plotted versus $\mathcal{E}$. This dependence reflects a higher electron temperature in the upper branch of the $n(\mathcal{E})$ characteristics leading to an impact ionization coefficient X_1, which differs by several orders of magnitude from the value on the lower and the middle branch. The decrease of T_e and X_1 in a small interval at the onset of the upper branch is due to electron cooling by impact ionization, mainly from the ground state, which is still highly occupied. For fields higher than about 10 V/cm impact ionization does no longer contribute to energy relaxation in a significant way since the donor ground states are almost completely ionized and impact ionization from the excited state, which is now more strongly populated than the ground state, dominates. Because of the much smaller energies involved, that process cools less efficiently and hence T_e and X_1 sharply rise. This is a threshold phenomenon which occurs at a critical value of n. The enhanced electron temperature for higher n supports the autocatalytic character of the impurity breakdown. Note that X_1^* does not show a strong dependence upon T_e because of the much smaller ionization energy and hence the values on the upper branch are not so much different from those on the lower and middle branch. The capture rate T_1^S decreases monotonically with the field (because fewer carriers are in states with small energies

TABLE I. Material parameters for n-type GaAs at $T_L = 4.2$ K used in the simulations.

Parameter	Value
lattice temperature	$T_L = 4.2$ K
relative static dielectric constant	12.9
effective mass	$0.067m_0$
lattice constant	5.64×10^{-10} m
crystal density	$5.36\ \mathrm{g\,cm^{-3}}$
acoustic deformation potential	5.0 eV
sound velocity	$5.24 \times 10^5\ \mathrm{cm\,s^{-1}}$
equivalent donor concentration	$N_D = 7.0 \times 10^{15}\ \mathrm{cm^{-3}}$
equivalent acceptor concentration	$N_A = 2.0 \times 10^{15}\ \mathrm{cm^{-3}}$
energy of donor ground state	$E_{t_1} = 5.839 \times 10^{-3}$ eV
energy of donor "effective" excited state	$E_{t_2} = 6.0 \times 10^{-5}$ eV
equilibrium recombination coefficient	$T_1^{S^0} = 4.5 \times 10^{-6}\ \mathrm{cm^3\,s^{-1}}$
equilibrium generation rate	$X_1^{S^0} = 1.17 \times 10^6\ \mathrm{s^{-1}}$
equilibrium impact ionization coefficient of excited state	$X_1^{*0} = 6.6 \times 10^{-6}\ \mathrm{cm^3\,s^{-1}}$
transition rate ground state to excited state	$X^* = 3.36 \times 10^5\ \mathrm{s^{-1}}$
transition rate excited state to ground state	$T^* = 4.1 \times 10^7\ \mathrm{s^{-1}}$

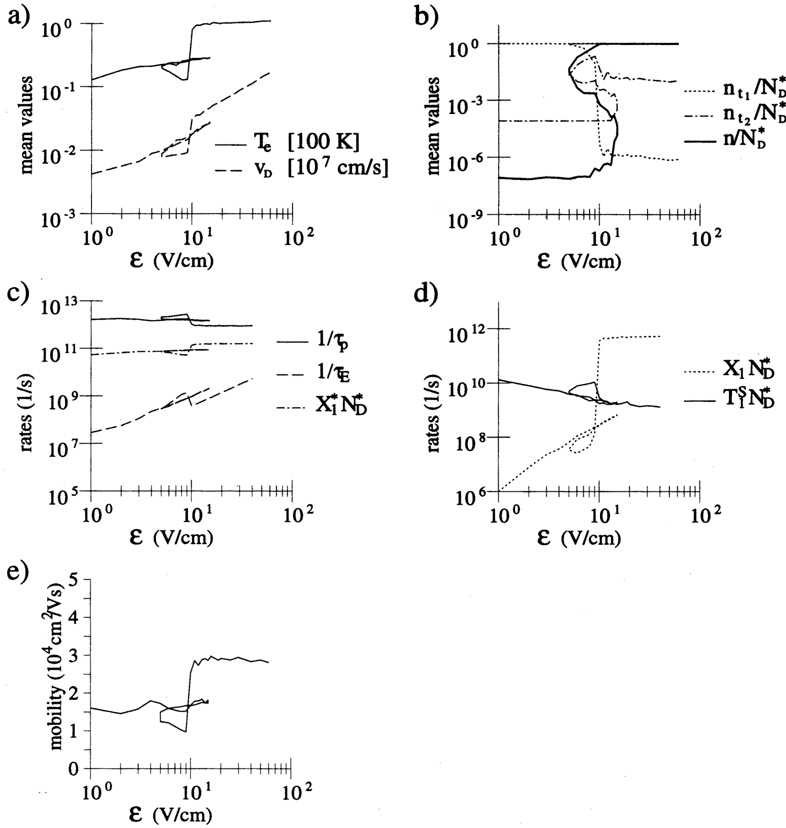

FIG. 3. (a) Electron temperature T_e (expressed in units of 100 K), and drift velocity v_D (in units of 10^7 cm/s); (b) carrier concentration in the donor ground state n_{t_1}, excited state n_{t_2}, and conduction band n (in units of the effective donor concentration $N_D^* \equiv N_D - N_A$); (c) inverse momentum (τ_p^{-1}) and energy (τ_E^{-1}) relaxation times, (c) and (d) impact ionization coefficients from the ground level (X_1) and the excited level (X_1^*), and the recombination coefficient T_1^S; (e) mobility for homogeneously doped GaAs at 4.2 K (single-particle MC simulation with the parameters of Table I).

from where they can recombine with high probability; see Fig. 1), except at the onset of the upper branch where T_1^S increases because strong impact ionization scatters many carriers back to the band minimum where they have a larger recombination probability. The drift velocity v_D generally increases with the field. On the upper branch, the mobility first drops below that of the lower and middle branch, but then exceeds it as a result of the sharp increase of carrier temperature and density around $\mathcal{E} = 10$ V/cm. This offers a consistent explanation of the anomalously high mobilities which were recently observed inside current filaments in n-GaAs,[9] as compared to the much lower mobilities outside.

IV. WEIGHTED ENSEMBLE MONTE CARLO METHOD

To model the experiment described in Ref. 10 we have performed EMC simulations for a sample where Si donors are arranged in δ layers spaced at $d = 100$ nm and completely ionized compensating Be acceptors are homogeneously distributed in the volume. The electric field is applied parallel to the δ layers. We simulate a section of one layer, assuming periodic boundary conditions. Space is discretized along the x axis perpendicular to the δ layers. In contrast to the homogeneous case (Sec. III), where a single-particle simulator has been used, coupling of charge carriers via Poisson's equation in the δ-doped structure requires the simultaneous simulation of an ensemble of particles and therefore the use of an EMC technique. The lateral electric field $\mathcal{E}_x$ to which the simulated particles are subjected consists of two parts. Due to the spatial separation of acceptors and donors a lateral electric field caused by space charges ρ_0 exists, which remains constant during the simulation. A second, time-dependent contribution is due to the diffusion of free car-

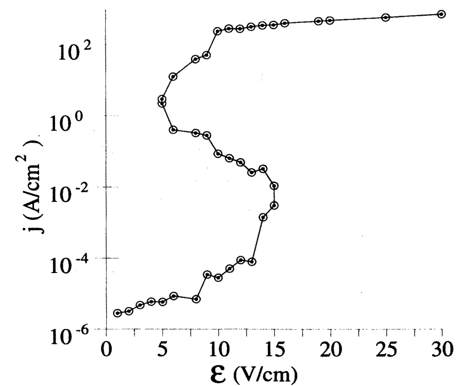

FIG. 4. Current density versus the electric field obtained from the Monte Carlo simulation for homogeneously doped GaAs (parameters as in Table I).

riers and is calculated self-consistently throughout the simulation. Integration of Poisson's equation yields, for the electric field in the middle of the ith box,

$$\mathcal{E}_x^i = \mathcal{E}_x^0 + \frac{1}{\epsilon\epsilon_0}\left(\frac{1}{2}\rho^i l^i + \sum_{j=1}^{i-1}\rho^j l^j\right). \tag{8}$$

Here l^i is the length, ρ^i is the total space charge density of the ith cell along the x axis, and ϵ, ϵ_0 are the relative and absolute permittivity. $\mathcal{E}_x^0$ is the electric field at the boundary of the sample ($x = 0$). ρ^i is composed of two parts

$$\rho^i = \left(\frac{\mathcal{N}_D^{*i}}{V_\delta} - n^i - n_{t_2}^i - n_{t_1}^i\right)e + \rho_0^i, \tag{9}$$

with

$$\mathcal{N}_D^{*i} = \begin{cases} \mathcal{N}_D^* & \text{in the } \delta\text{-doped layer} \\ 0 & \text{elsewhere,} \end{cases} \tag{10}$$

where n^i, $n_{t_2}^i$, and $n_{t_1}^i$ are the carrier densities in the conduction band, the excited levels, and the ground level in the ith cell. $\mathcal{N}_D^* = V(N_D - N_A)$ is the total number of available carriers, V is the volume of the simulated section of the sample, and V_δ is the volume of the δ layer. N_D and N_A are the equivalent donor and acceptor concentrations of the homogeneous case, respectively.

A MC simulation in the breakdown regime faces the severe problem that impurity breakdown is determined by the slow time scales connected with electronic transitions between donor ground states and excited states, and thermal generation (e.g., transient times of about 100 μs were reported in experiments[10]), while intraband scattering takes place on a femtosecond time scale. To overcome this difficulty we follow Ref. 15, where the slow processes were treated by deterministic rate equations and MC simulation was only performed for free carriers. Thus fluctuations due to transitions between donor levels and due to thermal generation do not appear in the simulation and bad statistics are avoided. Carrier number fluctuations due to recombination and impact ionization processes, however, do appear in the simulation.

A second problem arises as the concentration of free carriers can change by several orders of magnitude during the simulation due to impact ionization processes in the δ layer. Also δ doping may lead to large gradients of the carrier density in the direction perpendicular to the layers, resulting in poor statistics for those regions of the sample which are less visited by electrons. To solve that problem we made use of a weighted ensemble Monte Carlo technique.[29] Extending the method previously used for homogeneously doped p-germanium, the simulated particles represent time-dependent weights G_{ij}, according to

$$V(n_{t_2} + n_{t_1}) + \sum_{i=1}^{\mathcal{N}_{\text{sub}}}\sum_{j=1}^{\mathcal{N}_i} G_{ij}(t) = \mathcal{N}_D^*. \tag{11}$$

Here $\mathcal{N}_{\text{sub}}$ is the total number of subensembles along the x axis, $\mathcal{N}_i$ is the number of simulated quasiparticles in subensemble i, and $G_{ij}(t)$ is the time-dependent statistical weight of quasiparticle i in box j. If the number $\mathcal{N}_i$ of quasiparticles in a subensemble falls below a minimum value ($\mathcal{N}_i < 0.9\mathcal{N}_i^0$) or exceeds a maximum value ($\mathcal{N}_i > 1.1\mathcal{N}_i^0$), this subensemble is replaced by a statistically equivalent ensemble of $\mathcal{N}_i^0$ quasiparticles making use of a procedure described in Ref. 30.

V. CURRENT FILAMENTATION IN δ-DOPED GaAs

In order to avoid the long transient times associated with impurity breakdown in δ-doped GaAs,[10] we use the results obtained in Sec. III from a single-particle MC simulation for *homogeneously* doped GaAs as initial conditions in the δ layer (Fig. 3). In this simulation the *number* of donors in the δ layers is homogeneously distributed in the volume to obtain an equivalent situation. The simulations for homogeneous material yield an S-shaped $n(\mathcal{E})$ relation and thus reproduce the experimentally observed S-shaped current-field characteristics.

For an electric field $\mathcal{E} = 10$ V/cm, Fig. 5 shows the spatial distribution of free electron densities and temperatures perpendicular to the current flow and the transverse electric field $\mathcal{E}_x$ due to space charges as a function of time for δ-doped GaAs. For initial values corresponding to the lower branch [Fig. 5(a)], a well defined current filament (depicted by the carrier density and temperature profiles) is formed around the δ-doped layer at $x = 50$ nm. The higher carrier temperature on the high conductivity branch [Fig. 5(b)], on the other hand, leads to a smeared-out, diffuse distribution of hot electrons over the whole sample. Our dynamical simulations show that the relaxation of spatial carrier distributions is fast compared to the time scales of the generation-recombination kinetics. In Fig. 5(a) the transverse electric field $\mathcal{E}_x$ is completely determined by the positive donor (in the δ layer) and negative acceptor (elsewhere) space charges ρ_0, whereas in Fig. 5(b), on the high conductivity branch, the free carrier densities are no longer negligible and lead to considerable distortions of the field $\mathcal{E}_x$.

In Fig. 6 free electron densities, electron temperatures, and the transverse electric field is plotted as a function of the applied electric field $\mathcal{E}$ for the upper and the lower branch of the current-field characteristics. On the lower branch [Fig. 6(a)], the carriers are heated only in a narrow zone around the δ layer, and a current filament is formed for $\mathcal{E} \gtrsim 9$ V/cm due to carrier multiplication by impact ionization. On the upper branch [Fig. 6(b)], a current filament also exists for lower values of the electric field in the range $6\,\text{V/cm} \lesssim \mathcal{E} \lesssim 9\,\text{V/cm}$. The smeared-out distribution of electrons for higher applied electric fields above about 9 V/cm tends to destroy bistability, as the relative number of ionizing carriers in the δ layer decreases, when the total number of free carriers in the whole sample increases during the breakdown. Consequently the bistability interval is reduced in δ-doped samples as compared to homogeneously doped material, in agreement with experiments.[10] Furthermore, our simulations show that electron temperatures in the δ layer

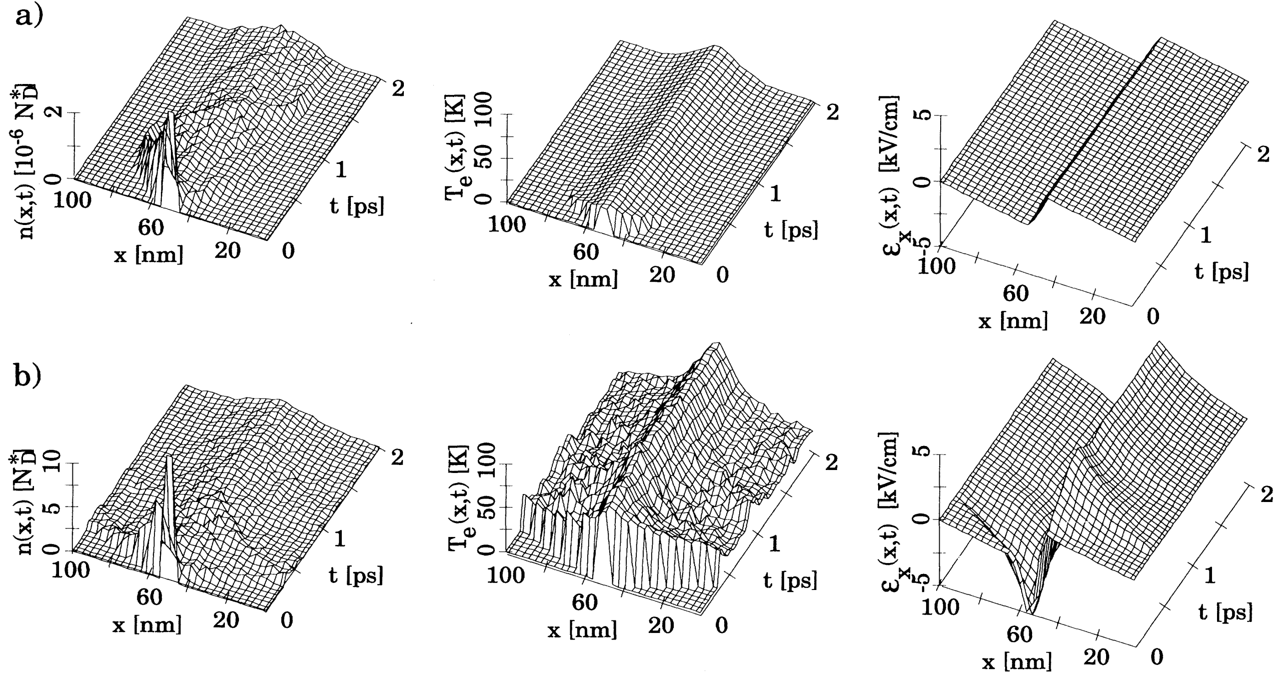

FIG. 5. Carrier density n, electron temperature T_e, and the transverse electric field $\mathcal{E}_x$ as a function of the transverse coordinate x and time t, corresponding (a) to the low conductivity and (b) to the high conductivity branch of the S-shaped homogeneous characteristic at $\mathcal{E} = 10$ V/cm ($N_D d = 7 \times 10^{10}$ cm^{-2}, $N_A = 2 \times 10^{15}$ cm^{-3}). The initial values for carrier concentrations and energies are chosen to be equal to the corresponding stationary values of the homogeneous characteristics within the δ-doped layer and zero elsewhere.

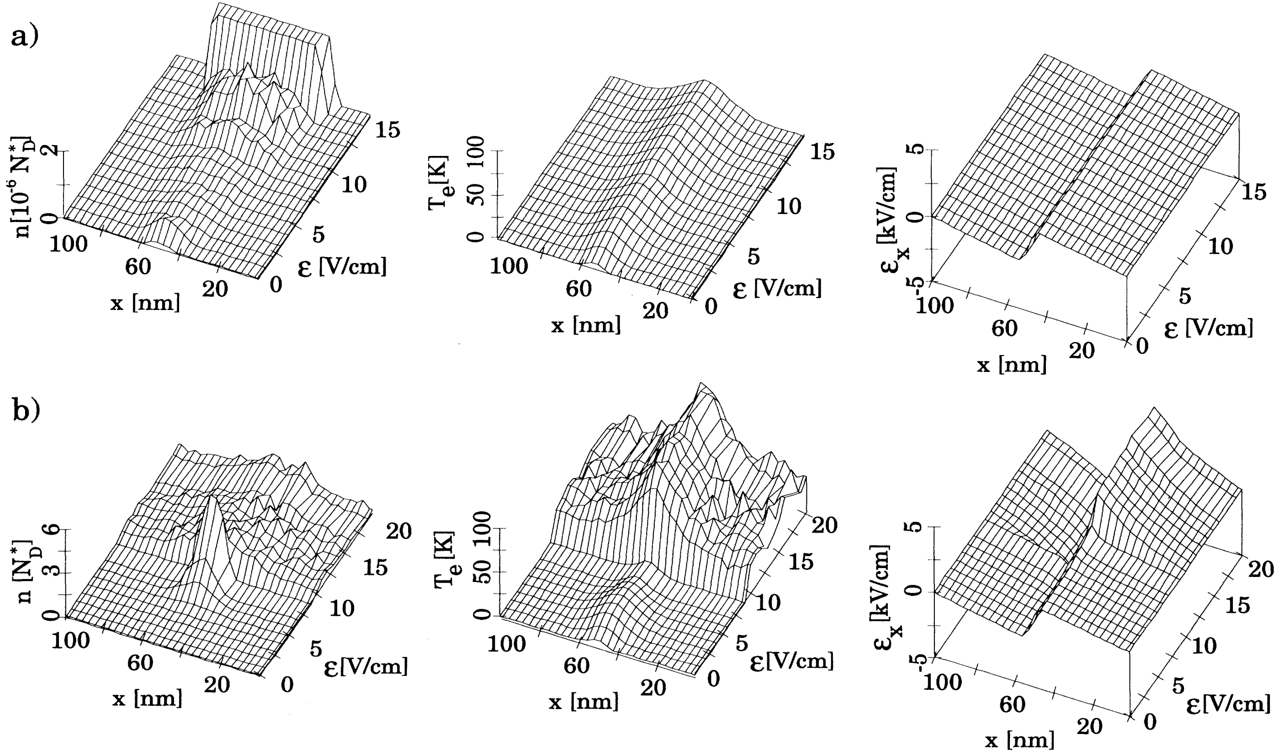

FIG. 6. Carrier density n, electron temperature T_e, and transverse electric field $\mathcal{E}_x$ as a function of the transverse coordinate x and the applied field $\mathcal{E}$ at $t = 2$ ps, corresponding (a) to the low conductivity and (b) to the high conductivity branch of the S-shaped homogeneous characteristic (parameters as in Fig. 5). The carrier density n in (a) is truncated for $n > 2 \times 10^{-6} N_D^*$. The initial values for carrier concentrations and energies are equal to the corresponding stationary values of the homogeneous characteristics within the δ-doped layer and zero elsewhere.

are higher as compared to the homogeneous case. This effect is due to the spreading of the carriers into the regions between the δ-doped layers where they experience reduced ionized impurity scattering and impurity impact ionization. Therefore the energy relaxation by impact ionization is weaker. The higher electron temperature in the δ layer for similar electric fields shifts the whole characteristic to lower voltages. This feature can also be observed in experiments.[10]

VI. CONCLUSIONS

We have presented a detailed microscopic analysis of breakdown and current filamentation in n-GaAs induced by impact ionization from shallow donors at liquid-helium temperature. First, we have calculated the carrier densities, electron temperatures, drift velocities, energy and momentum relaxation times, and impact ionization and capture rates from a single-particle Monte Carlo simulation for homogeneously doped material. By an iterative procedure we have achieved stable Monte Carlo simulations even in regimes which are dynamically unstable for fixed field. Thus we have been able to simulate directly the complete S-shaped current-field characteristics including the negative differential conductivity branch. A local minimum of the electron temperature due to cooling by impact ionization and a subsequent sharp rise for higher fields is found on the high conductivity branch, resulting in increased mobility and impact ionization rates with respect to the low conductivity branch. We have pointed out that the dependence of the GR coefficients not only upon the field, but also upon the carrier densities is crucial.

Second, we have presented an ensemble Monte Carlo simulation of a δ-doped GaAs sample in the regime of impurity breakdown. The spatial distribution of the carrier density, of the mean electron energy, and of the transverse electric field as a function of time has been calculated. Cooling by the impact ionization process was found to determine the shape of the spatial distribution of the carrier density. Reduced cooling for fields above about 9 V/cm on the upper branch of the current-field characteristic leads to a smeared-out distribution of the electrons over the sample and reduces the bistability interval. On the lower branch, and for smaller values of the electric field also on the upper branch, a current filament centered around the δ layer is formed. In the δ-doped layers higher electron temperatures as compared to the homogeneously doped sample arise as a result of reduced impurity scattering in the regions between the δ-doped layers and enhanced transverse space-charge fields due to the inhomogeneous doping. This shifts the whole characteristic to lower values, as observed in experiments.

ACKNOWLEDGMENTS

We wish to thank M. Asche, M. Gaa, H. Kostial, T. Kuhn, R. Kunz, D. Merbach, W. Prettl, and A. Wacker for valuable discussions. This work was supported by the Deutsche Forschungsgemeinschaft.

---

[1] G. E. Stillman, C. M. Wolfe, and J. O. Dimmock, *Semiconductors and Semimetals* (Academic, New York, 1977), Vol. 12.

[2] E. Schöll, *Nonequilibrium Phase Transitions in Semiconductors* (Springer, Berlin, 1987).

[3] K. Aoki, T. Kobayashi, and K. Yamamoto, J. Phys. (Paris) Colloq. **7**, C-51 (1981).

[4] A. Brandl, W. Kröninger, W. Prettl, and G. Obermair, Phys. Rev. Lett. **64**, 212 (1990).

[5] J. Spangler, U. Margull, and W. Prettl, Phys. Rev. B **45**, 12 137 (1992).

[6] E. Schöll, in *Handbook on Semiconductors*, edited by P. T. Landsberg, 2nd ed. (North Holland, Amsterdam, 1992), Vol. 1, pp. 419–447.

[7] J. Peinke, J. Parisi, O. E. Rössler, and R. Stoop, *Encounter with Chaos* (Springer, Berlin, 1992).

[8] G. Hüpper, K. Pyragas, and E. Schöll, Phys. Rev. B **47**, 15 515 (1993); **48**, 17 633 (1993).

[9] J. Spangler, B. Finger, C. Wimmer, W. Eberle, and W. Prettl, Semicond. Sci. Technol. **9**, 373 (1994).

[10] H. Kostial, M. Asche, R. Hey, K. Ploog, and F. Koch, Jpn. J. Appl. Phys. **32**, 491 (1993).

[11] E. Schöll, Z. Phys. B **46**, 23 (1982); **48**, 153 (1982).

[12] E. Schöll, Phys. Rev. B **34**, 1395 (1986).

[13] G. Hüpper and E. Schöll, Phys. Rev. Lett. **66**, 2372 (1991).

[14] T. Kuhn, G. Hüpper, W. Quade, A. Rein, E. Schöll, L. Varani, and L. Reggiani, Phys. Rev. B **48**, 1478 (1993).

[15] W. Quade, G. Hüpper, E. Schöll, and T. Kuhn, Phys. Rev. B **49**, 13 408 (1994).

[16] B. Kehrer, W. Quade, and E. Schöll, in *Proceedings of the 22nd International Conference on the Physics of Semiconductors, Vancouver, 1994*, edited by D. J. Lockwood (World Scientific, Singapore, 1995).

[17] P. J. van Hall and E. A. Zwaal, Superlatt. Microstruct. **13**, 323 (1993).

[18] K. Kometer, G. Zandler, and P. Vogl, Phys. Rev. B **46**, 1382 (1992).

[19] C. Jacoboni and L. Reggiani, Rev. Mod. Phys. **55**, 645 (1983).

[20] C. Jacoboni and P. Lugli, *The Monte Carlo Method for Semiconductor Device Simulation* (Springer, Wien, 1989).

[21] H. Kostial, Th. Ihn, P. Kleinert, R. Hey, M. Asche, and F. Koch, Phys. Rev. B **47**, 4485 (1993).

[22] A. A. Kastalsky, Phys. Status Solidi **15**, 599 (1973).

[23] The "effective" excited state arises from averaging over the energy loss and gain rates by GR processes involving a spectrum of n excited levels. The average is performed under nonequilibrium conditions.

[24] L. V. Keldysh, Zh. Eksp. Teor. Fiz. **37**, 713 (1959) [Sov. Phys. JETP **10**, 509 (1960)].

[25] M. Lax, Phys. Rev. **119**, 1502 (1960).
[26] V. N. Abakumov and I. N. Yassievich, Zh. Eksp. Teor. Fiz. **71**, 657 (1976) [Sov. Phys. JETP **44**, 345 (1976)].
[27] L. Reggiani and V. V. Mitin, Rev. Nuovo Cimento **12** (11), 1 (1989).
[28] A. Brandl and W. Prettl, Phys. Rev. Lett. **66**, 3044 (1991).
[29] F. Rossi, P. Poli, and C. Jacoboni, Semicond. Sci. Technol. **7**, 1017 (1992).
[30] R. Thoma, H. J. Peifer, W. L. Engl, W. Quade, R. Brunetti, and C. Jacoboni, J. Appl. Phys. **69**, 2300 (1991).